Catena 172 (2019) 65–75

Contents lists available at ScienceDirect

Catena

journal homepage: www.elsevier.com/locate/catena

Evaluation of static and dynamic land use data for watershed hydrologic process simulation: A case study in Gummara watershed, Ethiopia

Achenafi Teklay[a,*], Yihun T. Dile[b], Shimelis G. Setegn[c], Solomon S. Demissie[c], Dereje H. Asfaw[d]

[a] Ethiopian Institute of Water Resources, Department of Water Resources Engineering and Management, Addis Ababa University, Addis Ababa, Ethiopia
[b] Spatial Science Laboratory, Ecosystem Science and Management Department, Texas A & M University, College Station, TX 77801, USA
[c] Department of Earth and Environment, Florida International University, Miami, FL, USA
[d] Addis Ababa Institute of Science Technology, School of Environmental and Civil Engineering, Addis Ababa University, Addis Ababa, Ethiopia

ARTICLE INFO

Keywords:
Dynamic land use
Static land use
Land use change
Hydrological model parameters
Hydrological response
SWAT model

ABSTRACT

Land Use Land Cover (LULC) change significantly affects hydrological processes. Several studies attempted to understand the effect of LULC change on biophysical processes; however, limited studies accounted dynamic nature of land use change. In this study, Soil and Water Assessment Tool (SWAT 2012) hydrological model and statistical analysis were applied to assess the impacts of land use change on hydrological responses such as surface runoff, evapotranspiration, and peak flow in Gummara watershed, Ethiopia. Moreover, the effects of static and dynamic land use data application on the SWAT model performance were evaluated. Two model setups, Static Land Use (SLU) and Dynamic Land Use (DLU), were studied to investigate the effects of accounting dynamic land use on hydrological responses. Both SLU and DLU model setups used the same meteorological, soil, and DEM data, but different land use. The SLU setup used the 1985 land use layer, whereas the DLU setup used 1985, 1995, 2005, and 2015 land use data. The calibration (validation) results showed that the model satisfactorily predicts temporal variation and peak streamflow with Nash Sutcliffe Efficiency (NSE) of 0.75 (0.71) and 0.73 (0.71) in the DLU and SLU setups, respectively. However, the DLU model setup simulated the detailed biophysical processes better during the calibration period. Both model setups equally predicted daily streamflow during the validation period. Better performance was obtained while applying the DLU model setup because of improved representation of the dynamic watershed characteristics such as curve number (CN2), overland Manning's (OV_N), and canopy storage (CANMX). Expansion of agricultural land use by 11.1% and the reduction of forest cover by 2.3% during the period from 1985 to 2015 increased the average annual surface runoff and peak flow by 11.6 mm and 2.4 m^3/s, respectively and decreased the evapotranspiration by 5.3 mm. On the other hand, expansion of shrubland by 1% decreased the surface runoff by 1.2 mm and increased the evapotranspiration by 1.1 mm. The results showed that accounting DLU into the SWAT model simulation leads to a more realistic representation of temporal land use changes, thereby improving the accuracy of temporal and spatial hydrological processes estimation.

1. Introduction

Land Use Land Cover (LULC) change is one of the major global environmental challenges to humanity. It significantly affected hydrological response (Wagner et al., 2016; Su et al., 2015), ecosystem services (Lawler et al., 2014), and climate processes. Memarian et al. (2014) and Gebremicael et al. (2013) showed that the expansion of agriculture land use causes a significant change in runoff and sediment load. Significant variation of evapotranspiration has occurred due to LULC and leaf area index change (Li et al., 2015). Land use change can lead to a significant change in groundwater recharge and base flow (Budiyanto et al., 2015), flood frequency and interval (Alexakis et al., 2014), peak runoff (Ahn et al., 2014), and total suspended sediment and nutrient concentration (Hwang et al., 2016). Moreover, the land use change affects local, regional and global climate system (Deng et al., 2013) and degrades the health of a wetland ecosystem (Alam et al., 2011). Land use change has been one of the main contributors to climate changes (Cao et al., 2015). On the other hand, climate change has also been affecting the land use system through changes in agricultural productivity and forest ecosystem (Wang et al., 2013).

* Corresponding author at: Ethiopian Institute of Water Resources, Department of Water Resources Engineering and Management, Akaki Campus, P. Box 1176, Addis Ababa University, Ethiopia.
E-mail address: ashenafi45@yahoo.com (A. Teklay).

https://doi.org/10.1016/j.catena.2018.08.013
Received 17 September 2017; Received in revised form 2 August 2018; Accepted 13 August 2018
Available online 18 August 2018
0341-8162/

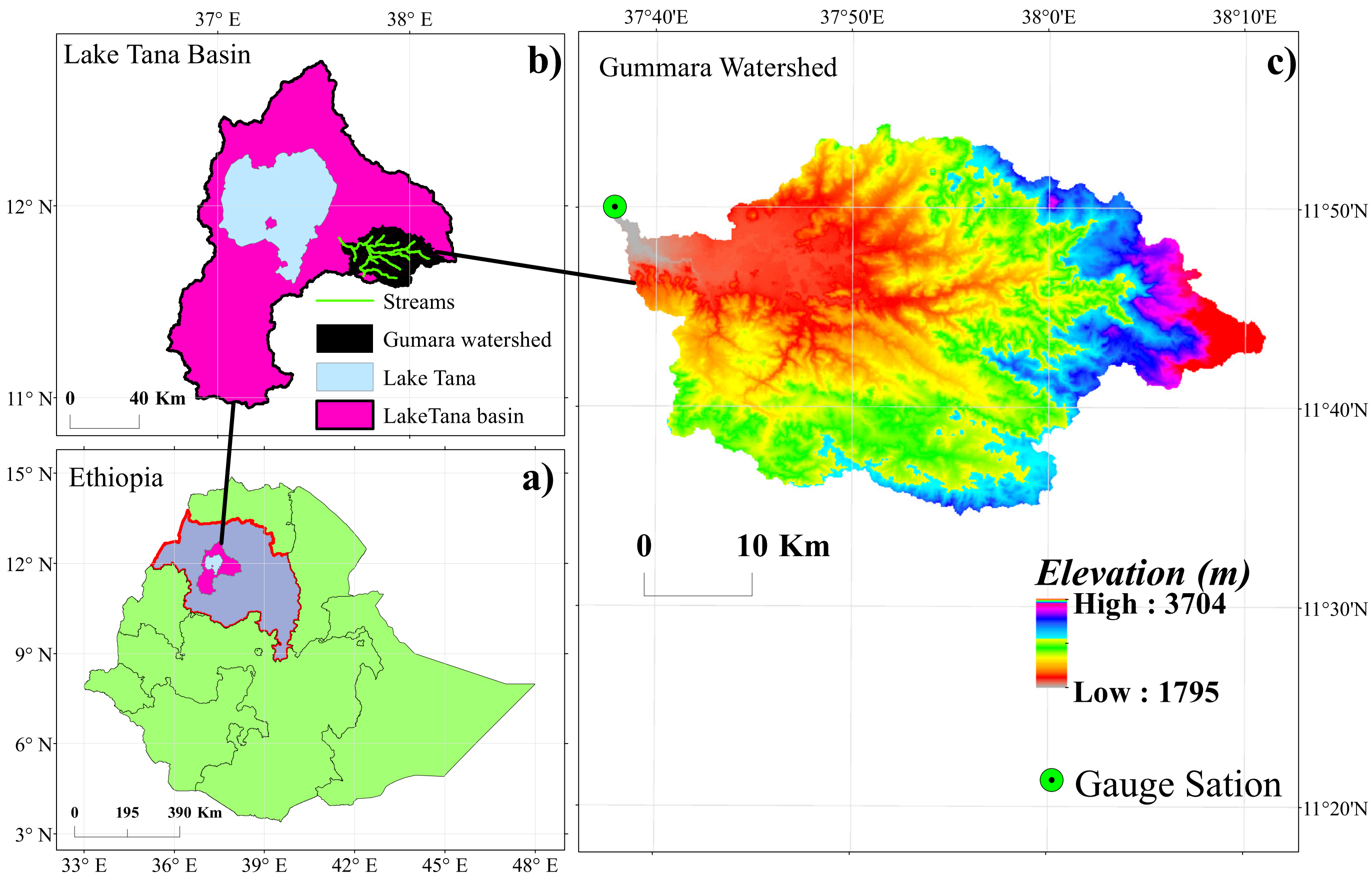

Fig. 1. Study watershed in the Lake Tana basin and Ethiopia. a) The location of the study watershed in the Amhara region (red border) and Ethiopia. b) Lake Tana basin showing the Gummera watershed in black border, and c) Gummara watershed zoomed with the elevation data as background.

Remote Sensing (RS), Geographic Information System (GIS), and hydrological modeling played a significant role in assessing the impact of land use change on different biophysical processes. RS data have played a major role in the watershed hydrological investigation (Ahn et al., 2014). LULC information derived from RS data has been used in a variety of hydrological modeling studies, especially in streamflow, water balance, flood event and soil erosion simulations (e.g., Dang and Kumar, 2017; Du et al., 2012). The GIS technology provided suitable alternatives for efficient management of large and complex databases. It also enhanced modeling efficiency and capability (Alexakis et al., 2014). For example, integration of the Soil and Water Assessment Tool (SWAT) with the GIS helped to understand the impacts of spatially explicit processes such as land use change on the hydrological response (Abbas et al., 2015; Yalew et al., 2013). Such tools have become vital for integrated river basin planning and management.

The SWAT model has strong track-record of evaluating the impacts of different land management practices on water budget, nutrient quantity and transport, and soil erosion in complex watersheds with varying soils, land uses, and management conditions over a long period of time (Arnold et al., 2012). For example, Briones et al. (2016) calibrated and validated SWAT model to study the impact of land use change on total water yields, groundwater, and base flow at sub-basin level in the Palico watershed in Batangas, Philippines. They showed that the combined forest and rangeland expansion by 22% increased base flow by 1–15%, and reduced streamflow by 1–17% in the rainy seasons. On the other hand, the reduction of forest cover by 54% decreased base flow between 11% and 17% in the rainy season, and increased surface runoff by 4–24%. Likewise, Huang and Lo (2015) applied the SWAT model to study the impacts of land use change on water budget and sediment losses over Yang Ming Shan National Park Watershed in northern Taiwan, and they reported that the conversion of forest land into agricultural land increased sediment loss.

Most SWAT model applications have been exclusively using static land cover data to study the effects of LULC change on watershed hydrologic modeling. Watershed processes represented by static land use data inadequately estimate the temporal and spatial hydrological variation (Wagner et al., 2016). Perhaps, use of dynamic land use (DLU) data may improve the spatial and temporal model simulation performance by capturing better the LULC evolution. Moreover, the DLU approach help to disaggregate the effects of land use change, climate variability and land management practices on the hydrological response (Fang et al., 2013; Chiang et al., 2010). Pai and Saraswat (2011) highlighted that stationarity in hydrological responses might happen in a single LULC application since such an approach simplifies the land use changes with time. Stationarity of hydrological responses can be resolved by integrating Land Use Change (LUC) modules into hydrological modeling approaches (Chiang et al., 2010; Saraswat et al., 2010). For example, Wagner et al. (2016) integrated SLEUTH land use change and the SWAT model, and they found sound seasonal and gradual changes in the water balance estimates. Similarly, Pai and Saraswat (2011), using LUC module with the SWAT model, improved the accuracy of estimation of the spatial and temporal hydrological fluxes such as surface runoff, groundwater, and evapotranspiration. However, several of these integrated LUC studies have the limitation of relying solely on model parameters derived from the calibration period, which uses static land use data. This approach overlooks the effects of land use changes on certain model parameters. For example, the study conducted by Gebremicael et al. (2013) showed there is a clear high discrepancy of calibrated model parameters between the 1973 and 2000 land use data for the 1971–1973 and 2000–2002 simulation periods, respectively. Since Gebremicael et al. (2013) uses different land use and climate data, the source of model parameter variation was unclear. In fact, limited studies assessed the isolated effect of LULC and climate change on hydrologic response. Unlike previous studies, this research applied the SWAT model using dynamic and static land use data to assess the effect of land use change on the SWAT model performance and hydrological processes.

2. Materials and methods

2.1. Study area

This study was conducted in Gummara watershed, in the eastern part of the Lake Tana Basin (Fig. 1). The watershed has an area of 1269 km^2, and is located in Amhara region, Ethiopia, between 37.63° to 38.18° longitude and 11.57° to 11.90° latitude. The topography of the study area is generally flat to moderate slope where 60% of the area has an average slope < 15%. The elevation in the basin ranges between 1794 and 3704 m above sea level, with a mean elevation of 2272 m.

The majority of the watershed area is covered by cultivated land (92%), and the remaining area is covered by shrubs (3%), grassland (4%), and forest (1%). The most dominant soil type is Haplic Luvisols (64%) which is found in the midstream parts of the watershed. The second dominant soil is Eutric Vertisols which is found in the downstream parts. Chromic Luvisols mainly extends to downstream and upstream parts of the watershed. Eutric Fluvisols is the least common soil type (< 1%) in the watershed. The climate of the watershed is humid with a long-term average annual rainfall is 1387 mm. The long-term average daily minimum and maximum temperatures are 9 °C and 28.5 °C, respectively. The average daily streamflow ranges between 0.2 m^3/s and 397.5 m^3/s.

2.2. Land use land cover analysis

Remotely sensed satellite data for Lake Tana Basin were reclassified using ArcGIS 10.1 software. Satellite data included Landsat 5 TM, Landsat 7 ETM+, and Landsat 8 OLI images with WRS Path 169 and Row 52. Landsat 5 TM images were acquired on February 26, 1985, and February 06, 1995. While Landsat 7 ETM+ image was acquired on March 29, 2005, and Landsat 8 OLI on February 13, 2015. The images of February and March were used because of the minimum cloud cover and surface features changes during the dry months in the watershed. The Landsat images were obtained from the United States Geological Survey (USGS) Earth Resources Observation and Science (EROS) data center (http://espa.cr.usgs.gov). The image data has a resolution of 30 m with standard geometric, radiometric, and atmospheric correction. The un-scanned gaps in ETM+ were filled using standardized ordinary co-kriging method (Zhang et al., 2007). Absolute units of Top-Of-Atmosphere (TOA) reflectance bands were used to maintain consistency among the TM, ETM+ and OLI images (Chander et al., 2009).

Field campaigns were conducted to observe land use conditions and record GPS locations, which were used for supervised land use classification and accuracy test. Observations were made from 268 training locations where 108, 47, 57 and 56 were taken from cropland, forest, shrubland, and grassland, respectively. The majority of the field data (192 observation points) were used for classification, and the remaining (76) were used for the accuracy test. Of the 192 training locations, 77, 34, 42, and 39 were in the agriculture, forest, shrubs, and grassland, respectively. Maximum likelihood classifier algorithm was used for image classification based on data from training locations and visual interpretation of the images. The distribution and spectral homogeneity of the training location pixels were checked using a histogram, scatterplots, and spectral statistics. The pixels in the training location had a normal distribution, and it represented well the entire area. The LULC types were classified into four major classes such as agricultural land, grassland, shrubland, and forest since these are the dominant land use types in the highland parts of Ethiopia (Teferi et al., 2013). The accuracy of the classification was overall satisfactory with an accuracy of 84% and a Kappa coefficient of 0.81 (Tadele et al., 2017). Kappa coefficient measures the inter-rater agreement, where a value of > 0.80 represents almost a perfect agreement. The classified land use types were used as LULC data in the SWAT model. The LULC data of the years 1985, 1995, 2005, and 2015 were used to represent different land use regimes over the watershed during four periods: 1985–1989, 1990–1999, 2000–2009, and 2010–2015 (Gebrehiwot et al., 2013).

2.3. SWAT model inputs and setup

2.3.1. Input data

The SWAT model requires a Digital Elevation Model (DEM), land use, soil, and climate data to simulate different hydrological processes. The DEM data with a spatial resolution of 90 m was obtained from the Shuttle Radar Topographic Mission (SRTM) (http://srtm.csi.cgiar.org/SELECTION/inputCoord.asp). The land use maps for the year 1985, 1995, 2005, and 2015 were prepared as presented in Section 2.2. The soil data, including its physical and chemical properties, were collected from the Ethiopian Ministry of Water, Irrigation, and Energy (EMWIE) and International Soil Reference and Information Center (ISRIC) with a spatial resolution of 1 km (http://www.isric.org). Daily rainfall, minimum/maximum temperature, solar radiation and average humidity data for the period from 1982 to 2015 were collected from three Ethiopian National Meteorological Services Agency (ENMSA) stations over the watershed (i.e., Debretabore, Dera Hamusit, and Wereta).

2.3.2. SWAT model setup

This study applied the ArcSWAT-2012 (version 586) to assess the effect of Static Land Use (SLU) and Dynamic Land Use (DLU) data on the performance of SWAT model simulations. The two model setups (SLU and DLU) used similar input data, but different land use data. The SLU setup used only the 1985 land use data for the entire simulation period, whereas the DLU setup used 1985, 1995, 2005, and 2015 land use data to simulate the hydrologic process for the four periods (i.e., 1982–1989, 1990–1999, 2000–2009, and 2010–2015). These land use data were applied using the Land Use Update (LUU) tool of the SWAT DLU model setup. The 1985 land use data was used to define the Hydrological Response Units (HRUs) in both model setups since it represents the beginning phase of the model simulation period. Both model setups were calibrated and validated using observed streamflow. The calibrated model was used to study the impacts of land use change on the hydrological response in Gummara watershed.

The model setup produced 22 sub-basins and 651 HRUs. The HRU definition considers every parcel of land use, soil, and slope to account full representation of watershed (Arnold et al., 2012). The detailed procedures and algorithm of the SWAT LUU tool are presented in Pai and Saraswat (2011).

2.3.3. SWAT model calibration and validation

The SWAT model parameters were calibrated using the Sequential Uncertainty Fitting version 2 (SUFI-2) in the SWAT-CUP (SWAT Calibration and Uncertainty Program, Abbaspour et al., 2007). The SWAT SLU and DLU models were calibrated and validated using observed daily streamflow data at the Gummara river gauging station (Fig. 1). The models were calibrated for the period from 1982 to 2005 with three years of model warm up (Daggupati et al., 2015). The models were validated for the period from 2006 to 2015. The calibration considered 18 hydrological parameters (Table 2) based on literature recommendation in the watershed (e.g., Dile et al., 2016; Gebremicael et al., 2013; Setegn et al., 2008).

2.4. Evaluation of land use change effect on the hydrological response

The temporal and spatial impacts of land use change on the hydrological response such as surface runoff, peak flow, and evapotranspiration was studied using the SLU and DLU model setups splitting the time period 1985–2015 into four. The temporal variation was studied using four-time frames namely 1985–1989, 1990–1999, 2000–2009, and 2010–2015, which represent different LULC regimes in the watershed. The spatial hydrological responses at the sub-basin scale were also assessed in the 2010–2015 period. The condition represented between the DLU and SLU simulations were similar except the land use. Therefore, the difference between the two model setups (i.e., DLU – SLU) provides the difference in hydrological response because of changes in land use representation.

2.5. SWAT model performance evaluation

Model performance evaluation is necessary to examine the representation of the modeling process to the actual biophysical conditions. The Nash Sutcliffe Efficiency (NSE) and Percent Bias (PBIAS) were used to evaluate the performance of the model simulations. The NSE indicates how well the observed versus simulated data fit the 1:1 line (Eq. (1)). The NSE value theoretically ranges from $-\infty$ to 1. The NSE of 1 corresponds to a perfect match between observed and simulated values. Moriasi et al. (2007) suggested that a model simulation that provides the NSE value of 0.75–1, 0.65–0.75, 0.5–0.65, and < 0.5 are considered as a very good, good, satisfactory, and unsatisfactory model performance, respectively.

$$NSE = 1 - \left(\sum_{i=1}^{N} (X_{obs} - X_{sim})^2 / \sum_{i=1}^{N} (X_{obs} - \overline{X})^2\right) \tag{1}$$

The PBIAS (Eq. (2)) is commonly used to measure the average tendency that the simulated data is higher or smaller than the observed data. PBIAS value can be positive or negative, where the value of zero represents the best model simulation performance. Positive values indicate model underestimation bias, and negative values indicate model overestimation bias. PBIAS value of $< \pm 10\%$, $\pm 10\%$– $\pm 15\%$, $\pm 15\%$– $\pm 25\%$, and $\geq \pm 25\%$ indicates that the model performs very well, good, satisfactory, and unsatisfactory, respectively (Moriasi et al., 2007).

$$PBIAS = \left(\sum_{i=1}^{N} (X_{obs} - X_{sim}) / \sum_{i=1}^{N} X_{obs}\right) * 100 \tag{2}$$

where, X_{obs} is the observed streamflow data, X_{sim} is the simulated streamflow data, $\overline{X}$ is the mean of the observed streamflow data, and N is the total number of streamflow data.

3. Results and discussion

3.1. Land use land cover (LULC) change

The spatial distribution of major LULC classes for 1985, 1995, 2005, and 2015 are presented in Fig. 2. It can be observed that the agriculture land use coverage was dominant in the upstream, midstream, and downstream part of the watershed. However, the forest and shrubland use were found dispersedly in the upstream and midstream parts. In a visual examination of land use maps, it was evident that from 1985 to 2015, the area under forest and shrub diminished significantly in the midstream region. The area under different LULC categories in Gummara watershed for different time periods is presented in Table 1.

Agriculture was the predominant land use type in Gummara watershed, and it covered 80% in 1985 and 91% in 2015 (Table 1). The forest coverage of the area was very small which accounted for only 0.8% in 2015 and 3.1% in 1985 (Table 1). The time series analysis of the LULC maps in the years between 1985 and 2015 indicated expansion of agriculture land use and a reduction of forest and shrubland use.

A significant expansion of agricultural land use (~8%) occurred between 1985 and 1995, and a slight reduction (~0.2%) occurred between 1995 and 2005. On the other hand, the forest coverage diminished between 1985 and 2015, which accounted for 73% of the 1985 forest cover. This was equivalent to a clearing of ~45%, ~22%, and ~6% forest in 1985–1995, 1995–2005, and 2005–2015, respectively. For the period from 1985 to 2015, agricultural land use increased by 11% and forest cover decreased by 2.3%. This estimate is consistent with the previous findings in the highlands of Ethiopia (e.g., Biru et al., 2015; Rientjes et al., 2011; Teferi et al., 2010). The grassland and shrubland area changed with a wavy pattern.

3.2. SWAT model calibration and validation

The ranges for SWAT model parameters and their adjusted values for the SLU and DLU model setups are presented in Table 2. The initial minimum and maximum values were based on a recommendation from published literature in the basin (e.g., Dile et al., 2016; Gebremicael et al., 2013; Arnold et al., 2012; Setegn et al., 2008). The calibrated best model parameter values were different for the SLU and DLU model setups (Table 2) which was mainly because of the difference in the land use data between the two model setups. Curve number (CN2), Manning's "n" value for overland flow (OV-N), and maximum canopy storage (CANMX) model parameters highly related to the land use type. These parameters significantly affect surface runoff and evapotranspiration simulation in the SWAT model. CN2 model parameter decreased from its original value by 9.1% and 9.5% in the DLU and SLU setup, respectively. However, the OV_N and CANMAX model parameters in the SLU setup were large, compared to the DLU setup. The higher value of CN2 and the lower value of OV_N and CANMAX in the DLU setup associated with the expansion of agriculture and reduction of forest and shrubland use in the study period. These findings are in agreement with the work done by Gebremicael et al. (2013) in the Blue Nile basin, and Briones et al. (2016) in the Palico watershed. The groundwater deep percolation fraction (RCHRG_DP) value was higher in the SLU model setup, compared to the DLU model setup; which indicated that SLU setup simulated more groundwater storage. The higher RCHRG_DP value mainly related with the higher forest and shrub coverage in the SLU setup. The groundwater recharge depth parameter agrees with Nejadhashemi et al. (2011) study in the agricultural region of Michigan and Wisconsin. As a whole, the variance among these model parameters of both model setups consistently reflects differences in hydrological processes under different land use information.

The performance of the model was evaluated by comparing the simulated daily streamflow from the DLU and SLU model setups with the observed streamflow data. The model performance statistics for the calibration and validation periods are presented in Table 3. The NSE values of the DLU setup were 0.75 for the calibration period and 0.71 for the validation period, corresponding to model performance ratings (Moriasi et al., 2007) of very good and good, respectively. However, the model performance was good in the case of SLU setup calibration and validation with the NSE values of 0.73 and 0.71, respectively. Likewise, evaluation using the R^2 for the DLU model simulation in the calibration and validation period was 0.75 and 0.80, respectively. The SLU model calibration and validation had similar R^2 values (0.74). The higher R^2 for both model setups indicated a very good linear relationship between simulated and observed streamflow data. Positive values of PBIAS for DLU setup (5.3% for calibration and 29.1% for validation) and SLU setup (7.1% for calibration and 24.9% for validation) indicated a tendency for underestimation of daily streamflow. However, the low magnitude of PBIAS values corresponded to a performance rating of "very good" during the calibration period, and the high magnitude of PBIAS values corresponded to a performance rating of "unsatisfactory" during the validation period. The PBIAS result showed a very small accumulation of difference in streamflow volume between the simulated and observed data for the calibration period. But, the model simulation in the DLU and SLU setups had a significant underestimation tendency during the validation period. A more stringent test of model performance was found during the validation period since parameter

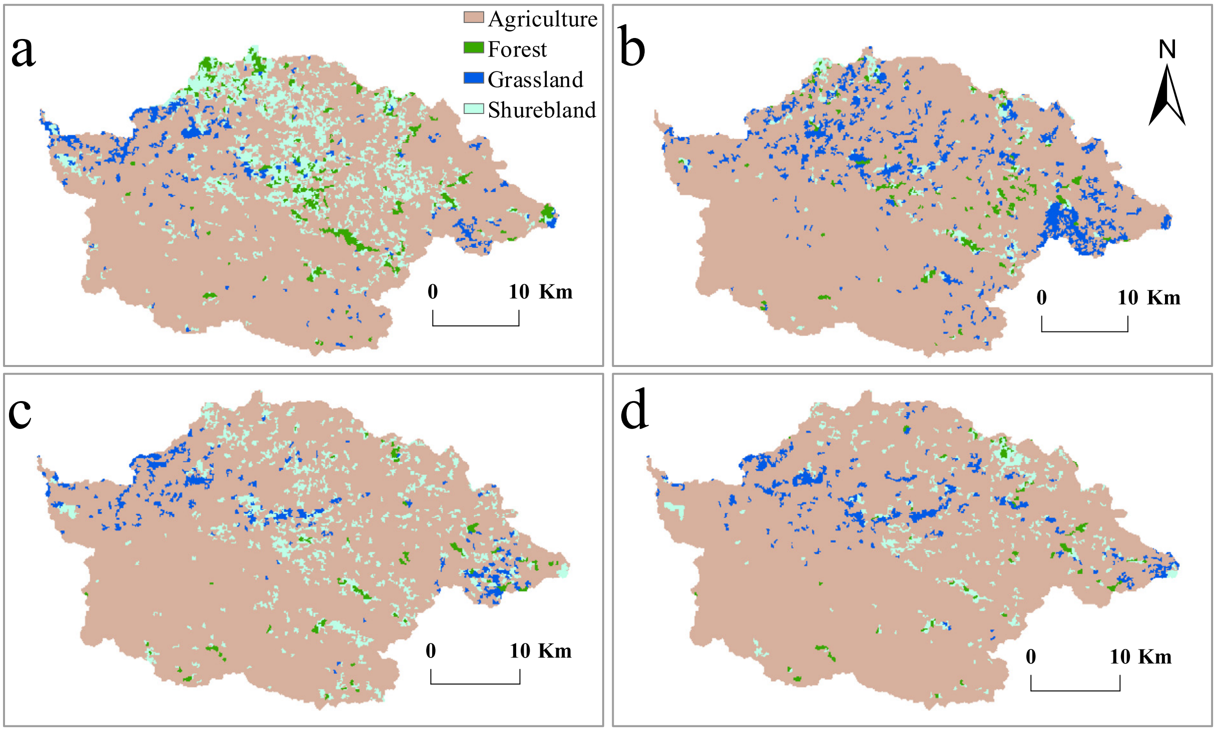

Fig. 2. Land use land cover maps of the Gummara watershed: land uses for a) 1985, b) 1995, c) 2005, and d) 2015.

range was fixed during this period (Saraswat et al., 2010). Therefore, according to the model evaluation criteria recommended by Moriasi et al. (2007), the performance of SLU and DLU SWAT model was satisfactory during the calibration period. This result agrees well with the previous studies in Gummara watershed (Dile et al., 2016; Setegn et al., 2008).

The P-factor and R-factor were estimated to evaluate the degree of uncertainty for both model simulations. P-factor is the percentage of the observed data covered by the 95% prediction of uncertainty (95PPU), and R-factor is the average thickness of the 95PPU band divided by the standard deviation of the observed data. The DLU model setup showed satisfactory model uncertainty during calibration (validation) period with P-factor of 0.87 (0.77) and R-factor of 0.65 (0.54). Comparable uncertainty level was found in the SLU model setup with P-factor of 0.87 (0.78) and R-factor of 0.64 (0.57) for calibration (validation) periods. The uncertainty factors showed acceptable model uncertainty estimates. According to Abbaspour et al. (2007) recommendation, P-factor ≥ 0.75 and R-factor ≤ 1.5 would be desirable for streamflow.

Simulated daily streamflow from SLU and DLU model setup were compared with observed values during the calibration and validation period (Fig. 3). Generally, there was a good agreement between the observed and simulated flows in both model setups, but a few peak flow events were not adequately captured during the rainy period. DLU and SLU simulated peak flow values were higher than observed values in July 29/1988, August 28/1999, August 22/2005 and August 04/2010

Table 2
Ranges for model parameter changes and best parameter values for SLU and DLU model setup for streamflow calibration. The SLU and DLU refer to the static land use and dynamic land use conditions, respectively.

S. N	Parameter name	Minimum value	Maximum value	DLU	SLU
1	r_CN2.mgt	−0.15	0.15	−0.091	0.095
2	v_ALPHA_BF.gw	0	0.5	0.40	0.25
3	v_GW_DELAY.gw	15	109	29.50	24.87
4	v_GWQMN.gw	0	10	5.75	0.45
5	v_ GW_REVAP.gw	0.1	0.2	0.10	0.13
6	v_RCHRG_DP.gw	0	0.88	0.06	0.15
7	v_GWHT.gw	0	10	8.90	1.45
8	v_REVAPMN.gw	0	10	9.85	8.15
9	r_SOL_AWC(..).sol	−0.13	0.11	−0.10	−0.09
10	r_SOL_K(..).sol	0.02	0.2	0.04	0.08
11	r_ESCO.hru	−0.15	0.15	−0.04	0.12
12	r_EPCO.hru	−0.15	0.15	0.03	−0.08
13	r_OV_N.hru	−0.15	0.15	−0.02	0.01
14	r_SLSUBBSN.hru	−0.15	0.15	−0.12	0.14
15	v_CANMX.hru	10	50	11.80	21.00
16	v_SURLAG.bsn	0	0.9	0.15	0.02
17	v_CH_N2.rte	0.02	0.3	0.15	0.15
18	v_CH_K2.rte	6	28	17.33	14.03

Note: "r_": relative change to the existing parameter value, i.e. the existing value is multiplied by 1 + a given value, and "v_": the existing parameter value is to be replaced by the given value.

Table 1
Land use land cover area percentage and changes for the 1985–2015 period in the Gummara watershed.

Land use type	Land use land cover (%)				Changes in land use land cover (%)		
	1985	1995	2005	2015	1985–1995	1995–2005	2005–2015
Agriculture	80.1	87.8	87.6	91.2	7.7	−0.2	3.6
Forest	3.1	1.7	1.0	0.8	−1.4	−0.7	−0.2
Grassland	3.6	7.8	3.2	3.6	4.2	−4.6	0.4
Shrubs	13.2	2.7	8.2	4.4	−10.5	5.5	−3.8
Total	100	100	100	100	0	0	0

Table 3
Goodness-of-fit evaluation statistical for the calibration and validation periods in SLU and DLU model setups.

Model setup		NSE	R^2	PBIAS	P-factor	R-factor
Dynamic Land Use (DLU)	Calibration	0.75	0.75	5.3	0.87	0.65
	Validation	0.71	0.80	29.1	0.77	0.54
Static Land Use (SLU)	Calibration	0.73	0.74	7.1	0.87	0.64
	Validation	0.71	0.74	24.9	0.78	0.57

(Fig. 3a and b), which mainly caused by the higher rainfall input during these periods. Both model setups had underestimation (61%) and overestimation (39%) tendency for the peak event simulation. The SLU and DLU simulated streamflow were consistently underestimated compared to observed values, in particular during 1990 to 1992, 1995 to 1997 and 2008 to 2009 (Fig. 3a and b).

Comparable goodness-of-fit and P-factor & R-factor values indicated that the model performance between DLU and SLU setup did not show a significant difference. Although the DLU setup did not show pronounced improvement, the calibration period DLU model setup performed slightly better than the SLU model setup. The higher NSE and R^2, and lower PBIAS value revealed the slightly better performance of the DLU model setup, which was mainly due to the better representation of the temporal land use changes in the DLU setup. During the validation period, both model setups were noticeably worse (lower NSE and higher PBIAS) than during the calibration period. Based on the similar values of NSE, both model setups were equally able to predict daily streamflow during the validation period. The PBIAS for both model setups did not agree with other criteria, and the values of DLU were higher than the SLU during the validation period. Wagner et al. (2017) and Pai and Saraswat (2011) also found improvement in model simulation by applying dynamic land use data.

3.3. Hydrological response under static and dynamic land use

3.3.1. Temporal variation of the hydrological response

The temporal land use effects on surface runoff, evapotranspiration, and peak flow were studied in the four periods where dynamic land use change was implemented. The hydrological responses with agricultural and forest land use percentage are summarized and presented in Table 4. The simulated hydrological processes from the SLU model setup were different between the four periods (1985–1999, 1990–1999, 2000–2009, and 2010–2015), which mainly associated with climate (rainfall) variations (Table 4). However, the hydrological responses difference in the DLU model setup related to climate variability and land use change. Therefore, the difference in the hydrological components between the SLU and DLU model setups provided the isolated impact of land use change.

The simulated surface runoff, evapotranspiration, and peak flow in the SLU and DLU model setups were similar in the 1985–1989 period, which used 1985 land use data. The estimated surface runoff, peak flow, and evapotranspiration in DLU and SLU setup were different in 1990–1999, 2000–2009, and 2010–2015 period, since the DLU model setup dynamically replaced the 1985 land use by 1995, 2005, and 2015 land use data during respective periods. In these periods, the DLU model setup simulated lower evapotranspiration and higher surface runoff and peak flow. The maximum and minimum variation of these hydrologic responses occurred in the 2010–2015 and 2000–2009

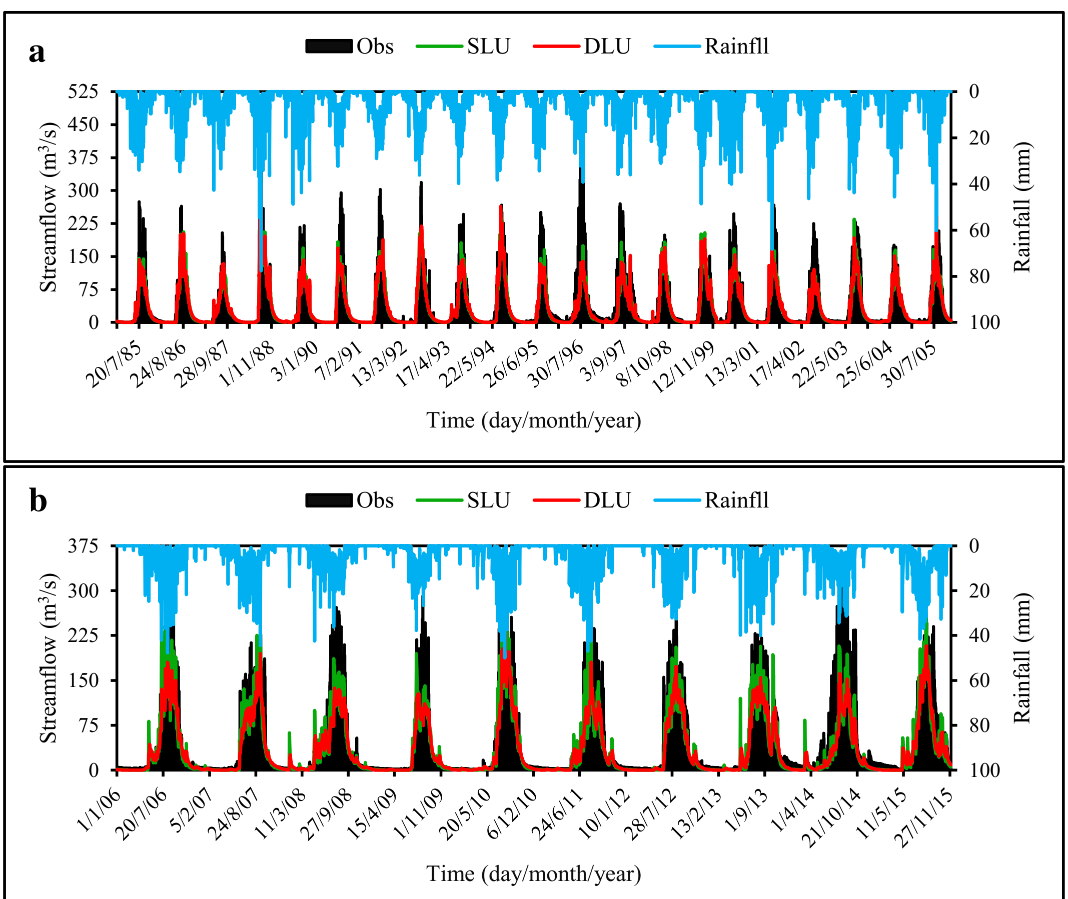

Fig. 3. Observed and simulated (DLU and SLU) daily streamflow for Gummara watershed during: a) calibration period (2006–2015), and b) validation period (2006–2015).

Table 4
The average hydrological response in the agricultural and forest land use types in the periods where static and dynamic land use was implemented.

Simulation period	Agricultural landuse (%)		Forest landuse (%)		PRECIP (mm)		SURQ (mm)		ET (mm)		Peak flow (m^3/s)	
	SLU	DLU	SLU	DLU	SLU	DLU	SLU	DLU	SLU	DLU	SLU	DLU
1985–1989	80.1	80.1	3.1	3.1	1443	1443	363.7	363.7	523.0	523.0	219.3	219.3
1990–1999	80.1	87.7	3.1	1.7	1387	1387	348.7	358.1	491.5	487.3	175.7	176.8
2000–2009	80.1	87.6	3.1	1.0	1332	1332	313.1	321.1	479.3	473.5	184.6	187.5
2010–2015	80.1	91.2	3.1	0.8	1435	1435	397.2	408.8	445.0	439.7	220.6	223.0

Note PRECIP: average annual precipitation (mm H_2O), SURQ: surface runoff (mm), ET: actual evapotranspiration (mm), SLU: static land use, and DLU: dynamic land use.

period, respectively. The maximum difference in surface runoff and peak flow between the two model setups were 11.6 mm and 2.4 m^3/s, respectively. This variation directly related to the agricultural land use expansion by 11.1% and forested area reduction by 2.3% in DLU model setup. Andualem and Gebremariam (2015) showed similar findings in Gilgal Abay watershed, Lake Tana basin. Likewise, Yin et al. (2017) found a similar experience in a semi-humid and semi-arid transition zone in northwest China. The simulated evapotranspiration values were lower in the DLU model setup mainly because of the consideration of low forest coverage, compared to SLU model setup. Higher evapotranspiration occurred in forested and vegetated watersheds (Alemu et al., 2014) due to higher transpiration and evaporation from the canopy (Getahun and Haj, 2015). This result agrees well with the study conducted by Fang et al. (2013) in Laohahe River basin, China. Their study showed that the expansion of vegetation cover areas decreased surface runoff and increased actual evapotranspiration.

Since the SLU model setup considered static land use data for the entire simulation period and ignored the temporal land use dynamics, but it can help to study the temporal climate variability. On the contrast, the DLU model setup captured both the land use and climatic dynamics. Therefore, the DLU model explained very well the effects of land use change on the temporal variation of the surface runoff, evapotranspiration and peak flow. The DLU setup used realistic past land use change conditions. As also stated by Wagner et al. (2016) and Chiang et al. (2010), the temporal components of land use change are assessed well in the dynamic land use setup. Thus, surface runoff, peak flow, and evapotranspiration were assumed to be more realistically estimated. The comparison between DLU and SLU surface runoff, peak flow and evapotranspiration in the four simulation period is shown in Fig. 4. The increasing of the magnitude of land use changes increased the magnitude of surface runoff, peak flow and evapotranspiration variation (Fig. 4). The contrast between the DLU and SLU setup indicated the influence of land use change between the two simulation periods. DLU surface runoff simulation increased by 45.1 mm between 1985–1989 and 2010–2015 period while the SLU setup increased the surface runoff simulation by 33.5 mm. The isolated land use change increased surface runoff by 11.6 mm, which accounted for 25.7% of the total surface runoff change (45.1 mm). The contrast between 1985–1989 and 2010–2015 simulation in the SLU setup indicated the influence of the climate variation. The climate variation increased surface runoff by 33.5 mm, which accounted for about 74.3% of the total surface runoff increment. The above results showed that land use change and climate variation during 1985–1989 and 2010–2015 increased surface runoff, but the contribution of land use change was smaller than that of climate variation. Between this simulation period, combined land use change and climate variation increased peak flow by 3.7 m^3/s, and the percent contributions were 64.9% (2.4 m^3/s) for the land use change and 35.1% (1.3 m^3/s) for the climate variability. The integrated effect of land use change and climate variability (DLU) decreased evapotranspiration by 83.3 mm. The evapotranspiration decreased by 78 mm due to climate variability while evapotranspiration decreased by 5.3 mm due to the land use change, accounting for 93.6% and 6.4% of the total integrated effect (83.3 mm), respectively. From the three hydrological response considered in this research, peak flow variation was highly sensitive to land use change in Gummara watershed.

3.3.2. Spatial variation of the hydrological response

The effect of sub-basin level land use change on the hydrological components was studied using simulations based on the 1985 and 2015 land use data. Sub-basin level land use change between 1985 and 2015 are presented in Fig. 5. During this period, the agricultural land use

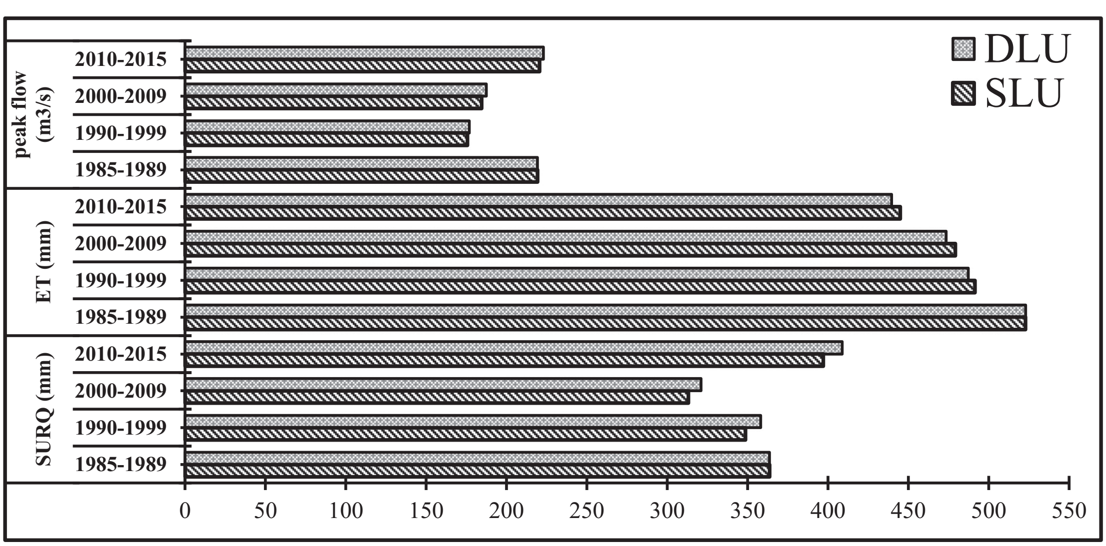

Fig. 4. Temporal comparison of SLU and DLU setup surface runoff, peak flow and evapotranspiration.

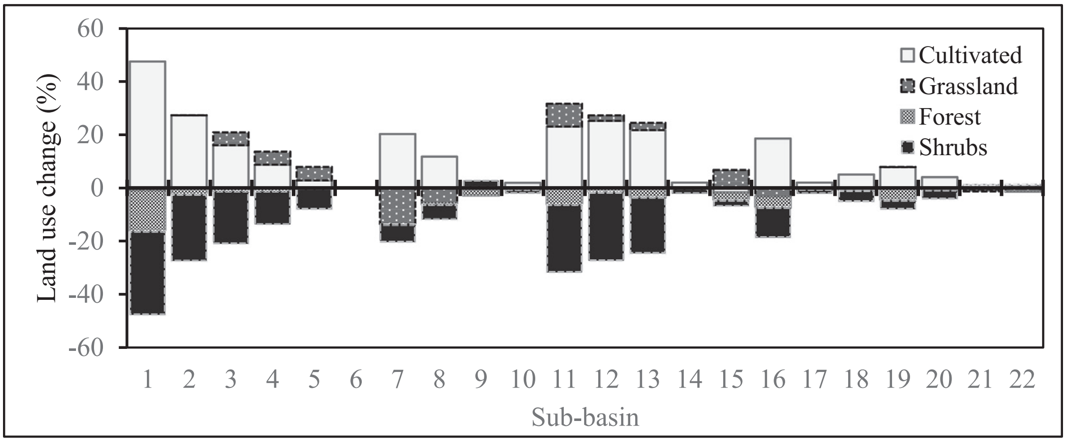

Fig. 5. Percentage of subbasin land use land cover change in the years between 1985 and 2015.

area increased in all sub-basins except in sub-basin 6, 9, 15, and 21 (Fig. 5), with the maximum expansion of 47.1% in sub-basin 1. The forest coverage slightly increased in sub-basin 21, whereas insignificant land use change was noticed in sub-basin 6.

The spatial impacts of land use change on the hydrological response were investigated using the average of SLU and DLU simulation in the 2010–2015 period. Sub-basin surface runoff, peak flow and evapotranspiration change between DLU and SLU setup are presented in Fig. 6. The magnitude and direction of the sub-basin level hydrological response change were assessed in relations to 1985 and 2015 land use data. Due to the expansion of agricultural land use and reduction of forest coverage in most of the sub-basins, higher surface runoff and peak flow were found in the DLU model setup. Sub-basin 1, 12, and 13, had the largest change of surface runoff, with a maximum increasing of 50.1 mm surface runoff (Fig. 6a). These maximum changes of surface runoff associated with the maximum expansion of agricultural land use by 47.5% in sub-basin 1. The expansion of shrubs and forest lands in sub-basin 9 and 21 resulted in the reduction of surface runoff. Shrubland expansion (2.5%) in sub-basin 9 decreased surface runoff (0.5 mm). Likewise, 1.1% expansion of forest coverage in sub-basin 21 decreased the surface runoff by 1.2 mm. Similar results about surface runoff increment due to the expansion of agricultural land use and the reduction of forest were reported in another region (Huang and Lo, 2015). As shown in Fig. 6b, the largest peak flow variation between DLU and SLU occurred in the downstream parts of the watershed (sub-basin 1, 5, 7, and 8) which may be due to the higher expansion of agricultural land use and reduction of forest land use over these sub-basins. The highest agricultural land use expansion (47.5%) caused higher peak flow (2.2 m^3/s) variation in sub-basin 1. The SLU simulation considered higher forest and shrub coverage during the 2010–2015 simulation period this caused the higher simulation of evapotranspiration, compared to DLU model setup. The largest change of evapotranspiration occurred in sub-basins 1, 2, 7, and 13, with a maximum decrease of 39.7 mm (Fig. 6c). A slightly higher forest coverage (1.1%) in the DLU model setup over sub-basin 21 caused 1.1 mm more evapotranspiration simulation, compared to SLU model setup. This result is consistent with Dias et al. (2015) studies where watersheds with an increase in forest cover tend to have higher evapotranspiration, and lower surface runoff and peak flow. As a result of static land use in sub-basin 6, there was an insignificant change in surface runoff, peak flow, and evapotranspiration.

The dynamic changes in land use and their spatial distribution were analyzed to assess the effects of land use change on surface runoff, peak flow, and evapotranspiration simulation in the selected sub-basins (Table 5). The DLU and SLU model setups were compared in 2010–2015 simulation period. In this period, the DLU setup used 2015 land use data, while the SLU setup used 1985 land use. Thus, the DLU setup considered the realistic representation of spatial land use coverage and their effects on hydrologic response. The curve number (CN2) is the most sensitive parameter in determining the fraction of precipitation converted to surface runoff (Briones et al., 2016). The alteration of land use between 1985 and 2015 affected the sub-basins CN2. The consideration of the actual expansion of agricultural land use in DLU setup caused a higher CN2 (sub-basin 1, 7, 10, 12, and 13), whereas the expansion of forest and shrubs resulted in a lower CN2 (sub-basin 21). The expansion of agricultural land use in sub-basin 1 caused the CN2 rise from 76.2 to 79.6, due to this the surface runoff and peak flow simulation increased from 285 mm to 335 mm and from 10.8 m^3/s to 13 m^3/s, respectively (Table 5). The result agrees with the findings of Dang and Kumar (2017) who reported that the higher the CN2 value, generated the higher the surface runoff and peak flow. The increase in surface runoff can be attributed to reduced evapotranspiration. Higher surface runoff and lower evapotranspiration are expected in agricultural land use than forest and shrubs area (Anaba et al., 2017). The static land use coverage in sub-basin 6 resulted in invariant CN2 and hydrological responses. Expansion of forest and shrubs coverage would result in an increase in the interception and infiltration opportunity time and thereby result in more water being infiltrated into the soil and decline the surface runoff. In the afforested sub-basin 21, high evapotranspiration was found mainly because of the higher transpiration and interception. Generally, the results showed that the consideration of the real land use change in the DLU setup produced the non-stationary hydrologic response. This finding agrees with the previous research result which indicated that land use dynamics causes of non-stationary hydrologic response (Ajami et al., 2017; Guse et al., 2015).

4. Conclusions

This study evaluated the impacts of Static Land Use (SLU) and Dynamic Land Use (DLU) on the representative hydrological processes using SWAT hydrological model. The SWAT model evaluation showed that the SLU and DLU setups affected the model parameters and the SWAT model performance. The SWAT model calibration under SLU and DLU setup provided satisfactory results during the calibration period. The DLU setup, which represented the 30 years' land use dynamics, had a higher curve number, and a lower canopy storage and groundwater recharge parameters due to the conversion of forest and shrubland into agricultural land. Statistical comparison between simulated and observed streamflow showed a slight model performance improvement in the case of dynamic land use setup.

The temporal and spatial analysis showed that implementing dynamic land use data affected the hydrological responses of Gummara watershed in terms of surface runoff, peak flow, and

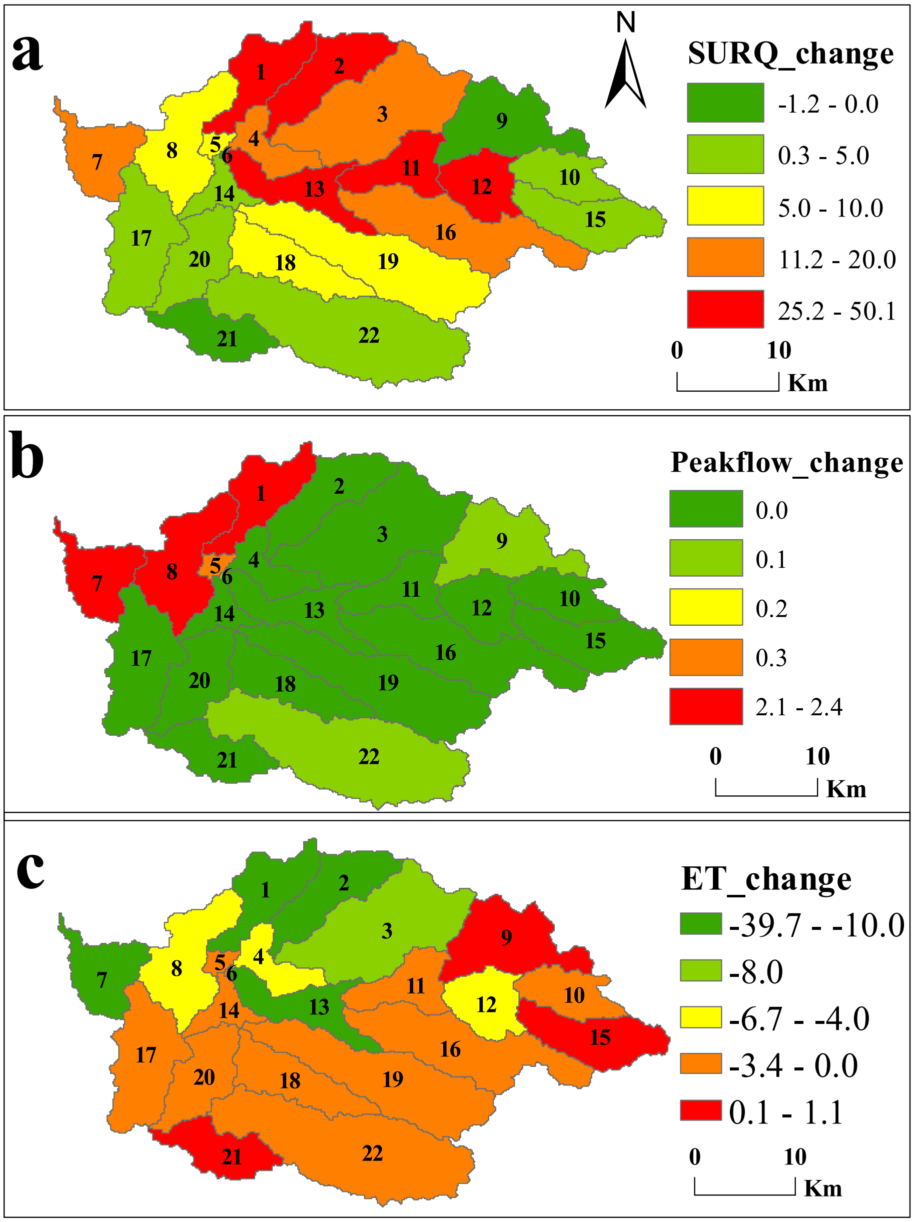

Fig. 6. Subbasin level change in hydrological response: change in a) surface runoff (SURQ, mm), b) peak flow (m^3/s) and c) evapotranspiration (ET, mm) between DLU and SLU model setups for the simulation period 2010–2015.

Table 5
Impact of LULC changes on surface runoff, peak flow and evapotranspiration in selected subbasins distributed in the upstream, midstream, and downstream areas of the watershed.

Sub-basin	Hydrological responses						Curve number (CN2)		Land use change between 1985 and 2015			
	SURQ (mm)		ET (mm)		Peak flow (m^3/s)				Agriculture	Forest	Grassland	Shrubs
	SLU	DLU	SLU	DLU	SLU	DLU	SLU	DLU				
1	285	335	563	523	10.8	13.0	76.2	79.6	48	−16	−1	−31
6	347	347	544	544	116	116	80.3	80.3	0	0	0	0
7	558	569	482	471	220	223	80.7	81.1	20	0	−14	−6
10	408	411	303	302	9	9	79.6	79.7	2	−1	0	−1
12	380	406	305	300	33	33	77.9	79.6	26	−2	2	−26
13	314	339	540	526	83	83	78.1	79.8	22	−4	3	−21
21	527	526	477	479	12	12	79.5	79.4	−0.5	1	−0.8	0.3

evapotranspiration. The average annual surface runoff and peak flow increased while the evapotranspiration decreased when the forest and shrubland area converted into agriculture land. However, the effects of land use change on the hydrological response were non-uniform over space and time. The DLU model setup can better represent the spatial and temporal variability of hydrologic processes caused by the temporal land use change. Sub-basins with an increase of agricultural land cover tend to increase surface runoff and peak flow, and a decrease of evapotranspiration. On the other hand, sub-basins with an increase in shrubs and forest land resulted in a decrease of surface runoff and an increase of evapotranspiration. The increase in surface runoff may have positive implications for irrigation activities since it can be harvested using water harvesting structures and used for crop production. On the other hand, an increase in surface runoff may also cause flooding problems for the surrounding area.

The findings from this study have shown that applying dynamic land use in the hydrological simulation improved model performance and thereby improve water resources estimations in watersheds. It can also help in implementing sustainable land and water management practices.

Acknowledgements

This work was supported by the International Foundation for Science [grant number W/5926-1]. This study would not have been possible without the support of basic software from Addis Ababa University and the University of Gondar. Ethiopian Meteorological Service Agency (EMSA), and the Ethiopian Ministry of Water, Irrigation, and Energy (EMWIE) supported by providing climate and hydrological data.

Appendix A. Supplementary data

Supplementary data to this article can be found online at https://doi.org/10.1016/j.catena.2018.08.013.

References

Abbas, T., Nabi, G., Boota, M.W., Hussain, F., Faisal, M., Ahsan, H., 2015. Impacts of landuse changes on runoff generation in Simly watershed. Sci. Int. 27, 3185–3191.
Abbaspour, K.C., Yang, J., Maximov, I., Siber, R., Bogner, K., Mieleitner, J., Zobrist, J., 2007. Modeling hydrology and water quality in the pre-alpine/alpine Thur watershed using SWAT. J. Hydrol. 333, 413–430.
Ahn, G., Gordon, S.I., Merry, C.J., 2014. Impacts of remotely sensed land use data on watershed hydrologic change assessment. Int. J. Geospat. Env. Res. 1, 1–15.
Ajami, H., Sharma, A., Band, L.E., Evans, J.P., Tuteja, N.K., Amirthanathan, G.E., Bari, M.A., 2017. On the non-stationarity of hydrological response in anthropogenically unaffected catchments: an Australian perspective. Hydrol. Earth Syst. Sci. 21, 281–294.
Alam, A., Rashid, S.M., Bhat, M.S., Sheikh, A.H., 2011. Impact of land use/land cover dynamics on Himalayan wetland ecosystem. J. Exp. Sci. 2, 60–64.
Alemu, H., Senay, G., Kaptue, A., Kovalskyy, V., 2014. Evapotranspiration variability and its association with vegetation dynamics in the Nile Basin, 2002–2011. Remote Sens. 6, 5885–5908.
Alexakis, D.D., Grillakis, M.G., Koutroulis, A.G., Agapiou, A., Themistocleous, K., Tsanis, I.K., Michaelides, S., Pashiardis, S., Demetriou, C., Aristeidou, K., Retalis, A., Tymvios, F., Hadjimitsis, D.G., 2014. GIS and remote sensing techniques for the assessment of land use change impact on flood hydrology: the case study of Yialias basin in Cyprus. Nat. Hazards Earth Syst. Sci. 14, 413–426.
Anaba, L.A., Banadda, N., Kiggundu, N., Wanyama, J., Engel, B., Moriasi, D., 2017. Application of SWAT to assess the effects of land use change in the Murchison Bay catchment in Uganda. Comput. Water Energy Environ. Eng. 6, 24–40.
Andualem, T.G., Gebremariam, B., 2015. Impact of land use land cover change on streamflow and sediment yield: a case study of Gilgel Abay watershed, Lake Tana. Int. J. Technol. Enhancements Emerg. Eng. Res. 3, 28–42.
Arnold, J.G., Moriasi, D.N., Gassman, P.W., Abbaspour, K.C., White, M.J., Srinivasan, R., Santhi, C., Harmel, R.D., van Griensven, A., Van Liew, M.W., Kannan, N., Jha, M.K., 2012. SWAT: model use, calibration, and validation. Trans. ASABE 55, 1491–1508.
Biru, M.K., Minale, A.S., Debay, A.B., 2015. Multitemporal land use land cover change and dynamics of Blue Nile basin by using GIS and remote sensing techniques, North-Western Ethiopia. Int. J. Environ. Sci. 4, 81–88.
Briones, R.U., Ella, V.B., Bantayan, N.C., 2016. Hydrologic impact evaluation of land use and land cover change in Palico watershed, Batangas, Philippines using the SWAT model. J. Environ. Sci. Manag. 19, 96–107.
Budiyanto, S., Tarigan, S.D., Sinukaban, N., Murtilaksono, K., 2015. The impact of land use on hydrological characteristics in Kaligarang watershed. Int. J. Sci. Eng. 8, 125–130.
Cao, Q., Yu, D., Georgescu, M., Han, Z., Wu, J., 2015. Impacts of land use and land cover change on regional climate: a case study in the agro-pastoral transitional zone of China. Environ. Res. Lett. 10, 1–13.
Chander, G., Markham, B.L., Helder, D.L., 2009. Summary of current radiometric calibration coefficients for Landsat MSS, TM, ETM+, and EO-1 ALI sensors. Remote Sens. Environ. 113, 893–903.
Chiang, L., Chaubey, I., Gitau, M.W., Arnold, J.G., 2010. Differentiating impacts of land use changes from pasture management in a CEAP watershed using the SWAT model. Trans. ASABE 53, 1569–1584.
Daggupati, P., Pai, N., Ale, S., Douglas-Mankin, K.R., Zeckoski, R.W., Jeong, J., Parajuli, P.B., Saraswat, D., Youssef, M.A., 2015. A recommended calibration and validation strategy for hydrologic and water quality models. Trans. ASABE 58, 1705–1719.
Dang, N., Kumar, L., 2017. Application of remote sensing and GIS-based hydrological modeling for flood risk analysis: a case study of District 8, Ho Chi Minh City, Vietnam. Geomat. Nat. Haz. Risk 8, 1792–1811.
Deng, X., Zhao, C., Yan, H., 2013. Systematic modeling of impacts of land use and land cover changes on regional climate: a review. Adv. Meteorol. 2013, 1–11.
Dias, L.C.P., Macedo, M.N., Costa, M.H., Coe, M.T., Neill, C., 2015. Effects of land cover change on evapotranspiration and streamflow of small catchments in the Upper Xingu River Basin, Central Brazil. J. Hydrol. 4, 108–122.
Dile, Y.T., Daggupati, P., George, C., Srinivasan, R., Arnold, J., 2016. Introducing a new open source GIS user interface for the SWAT model. Environ. Model. Softw. 85, 129–138.
Du, J., Qian, L., Rui, H., Zuo, T., Zheng, D., Xu, Y., Xu, C.Y., 2012. Assessing the effects of urbanization on annual runoff and flood events using an integrated hydrological modeling system for Qinhuai River basin, China. J. Hydrol. 464–465, 127–139.
Fang, X., Ren, L., Li, Q., Zhu, Q., Shi, P., Zhu, Y., 2013. Hydrologic response to land use and land cover changes within the context of catchment-scale spatial information. J. Hydrol. Eng. 18, 1539–1548.
Gebrehiwot, S.G., Seibert, J., Gardenas, A.I., Mellander, P., Bishop, K., 2013. Hydrological change detection using modeling: half a century of runoff from four rivers in the Blue Nile Basin. Water Resour. Res. 49, 3842–3851.
Gebremicael, T.G., Mohamed, Y.A., Betrie, G.D., van der Zaag, P., Teferi, E., 2013. Trend analysis of runoff and sediment fluxes in the Upper Blue Nile basin: a combined analysis of statistical tests, physically-based models, and land use maps. J. Hydrol. 482, 57–68.
Getahun, Y.S., Haj, V.L., 2015. Assessing the impacts of land use-cover change on hydrology of Melka Kuntrie subbasin in Ethiopia using a conceptual hydrological model. Hydrol. Curr. Res. 6, 1–11.
Guse, B., Pfannerstill, M., Fohrer, N., 2015. Dynamic modelling of land use change impacts on nitrate loads in rivers. Environ. Process. 2, 575–592.
Huang, T., Lo, K., 2015. Effects of land use change on sediment and water yields in Yang Ming Shan National Park, Taiwan. Environment 2, 32–42.
Hwang, S.A., Hwang, S.J., Park, S.R., Lee, S.W., 2016. Examining the relationships between watershed urban land use and stream water quality using linear and generalized additive models. Water 8, 1–15.
Lawler, J., Lewis, D.J., Nelson, E., Plantinga, A.J., Polasky, S., Withey, J.C., Helmers, D.P., Martinuzzi, S., Pennington, D., Radeloff, V.C., 2014. Projected land-use change impacts on ecosystem services in the United States. PNAS 111, 7492–7497.
Li, Y., Fan, J., Hu, Z., Shao, Q., Zhang, L., Yu, H., 2015. Influence of land use patterns on evapotranspiration and its components in a temperate grassland ecosystem. Adv. Meteorol. 2015, 1–12.
Memarian, H., Balasundram, S.K., Abbaspour, K.C., Talib, J.B., Sung, C.T.B., Sood, A.M., 2014. SWAT-based hydrological modeling of tropical land-use scenarios. Hydrol. Sci. J. 59, 1808–1829.
Moriasi, D.N., Arnold, J.G., Van Liew, M.W., Binger, R.L., Harmel, R.D., Veith, T.L., 2007. Model evaluation guidelines for systematic quantification of accuracy in watershed simulations. Trans. ASABE 50, 885–900.
Nejadhashemi, A.P., Wardynski, B.J., Munoz, J.D., 2011. Evaluating the impacts of land use changes on hydrologic responses in the agricultural regions of Michigan and Wisconsin. Hydrol. Earth Syst. Sci. 8, 3421–3468.
Pai, N., Saraswat, D., 2011. SWAT2009_LUC: a tool to activate land use change module in SWAT2009. Trans. ASABE 54, 1649–1658.
Rientjes, T.H.M., Haile, A.T., Kebede, E., Mannaerts, C.M.M., Habib, E., Steenhuis, T.S., 2011. Changes in land cover, rainfall and streamflow in Upper Gilgel Abbay catchment, Blue Nile basin - Ethiopia. Hydrol. Earth Syst. Sci. 15, 1979–1989.
Saraswat, D., Pai, N., Daniels, M., 2010. Identifying priority subwatersheds using distributed modeling approach. In: Chaubey, I., Yagow, G. (Eds.), Proc.TMDL 2010 Watershed Management to Improve Water Quality Conf. (ASABE Publication No. 711P0710cd).
Setegn, S.G., Srinivasan, R., Dargahi, B., 2008. Hydrological modelling in the Lake Tana basin, Ethiopia using SWAT Model. Open Hydrol. J. 2, 49–62.
Su, Z.H., Lin, C., Ma, R.H., Luo, J.H., Liang, Q.O., 2015. Effect of land use change on lake water quality in different buffer zones. Appl. Ecol. Environ. Res. 13, 639–653.
Tadele, H., Mekuriaw, A., Selassie, Y.G., Tsegaye, L., 2017. Land use/land cover factor values and accuracy assessment using a GIS and remote sensing in the case of the Quashay Watershed in Northwestern Ethiopia. J. Nat. Res. Dev. 7, 38–44.
Teferi, E., Uhlenbrook, S., Bewket, W., Wenninger, J., Simane, B., 2010. The use of remote sensing to quantify wetland loss in the Choke Mountain range, Upper Blue Nile basin, Ethiopia. Hydrol. Earth Syst. Sci. 14, 2415–2428.
Teferi, E., Bewket, W., Uhlenbrook, S., Wenninger, J., 2013. Understanding recent land use and land cover dynamics in the source region of the Upper Blue Nile, Ethiopia: spatially explicit statistical modeling of systematic transitions. Agric. Ecosyst.

Environ. 165, 98–117.
Wagner, P.D., Bhallamudi, S.M., Narasimhan, B., Kantakumar, L.N., Sudheer, K.P., Kumar, S., Schneider, K., Fiener, P., 2016. Dynamic integration of land use changes in a hydrologic assessment of a rapidly developing Indian catchment. Sci. Total Environ. 539, 153–164.
Wagner, P.D., Bhallamudi, S.M., Narasimhan, B., Kumar, S., Fohrer, N., Fiener, P., 2017. Comparing the effects of dynamic versus static representations of land use change in hydrologic impact assessments. Environ. Model. Softw. 2017, 1–9.
Wang, X.Y., Zhao, C.Y., Jia, Q.Y., 2013. Impacts of climate change on forest ecosystems in Northeast China. Adv. Clim. Chang. Res. 4, 1–14.
Yalew, S., van Griensven, A., Ray, N., Kokoszkiewicz, L., Betrie, G.D., 2013. Distributed computation of large scale SWAT models on the Grid. Environ. Model. Softw. 41, 223–230.
Yin, J., He, F., Xiong, Y.J., Qiu, G.Y., 2017. Effects of land use/land cover and climate change on surface runoff in a semi-humid and semi-arid transition zone in northwest China. Hydrol. Earth Syst. Sci. 21, 183–196.
Zhang, C., Li, W., Travis, D., 2007. Gaps-fill of SLC-off Landsat ETM+ satellite image using a geostatistical approach. Int. J. Remote Sens. 28, 5103–5122.